EARTH'S CRYOSPHERE
SCIENTIFIC JOURNAL

Earth's Cryosphere, 2023, vol. XXVII, No. 1, pp. 12–20

PHYSICAL AND CHEMICAL PROCESSES IN FROZEN GROUND AND ICE

RESULTS OF PHYSICAL MODELING OF SOIL FREEZING

V.G. Cheverev[1,*], A.V. Brushkov[1], E.V. Safronov[1], Yu.A. Kaynov[2], A.L. Fedotov[2]

[1] *Lomonosov Moscow State University, Leninskie Gory 1, Moscow, 119991 Russia*
[2] *Research Institute of Pipeline Transport, Sevastopolsky prosp. 47a, Moscow, 117186 Russia*

**Corresponding author; e-mail: cheverev44@mail.ru*

The article presents the results of physical modeling of soil freezing in laboratory. The samples of silty clay of kaolinite composition were used as model soil. The main characteristics of the component and phase composition of water, as well as the heat and mass transfer and deformation properties of the soil were experimentally determined. During the physical modeling, parameters of the freezing process, differential heaving of frozen and shrinkage of thawed zones, heat and moisture transfer, and pore pressure were monitored. The appearance of segregated ice in the freezing soil, layered axial and horizontal deformation, and the dynamics of density and water content of water-saturated soil samples over time were determined using position markers and time-lapse video.

Keywords*: physical modeling, freezing, heaving, characteristics of silty clay, process parameters.*

Recommended citation: Cheverev V.G., Brushkov A.V., Safronov E.V., Kaynov Yu.A., Fedotov A.L., 2023. Results of physical modeling of soil freezing. *Earth's Cryosphere* XXVII (1), 12–20.

INTRODUCTION

Frost heaving of freezing soils is a widespread dangerous geocryological process for buildings and engineering structures in the permafrost region of Russia [*Garagulya et al., 2000*]. In this regard, the forecast and management of this process are relevant.

Currently, despite many years of studies into the mechanism and regularities of the heaving process, the problem of developing a mathematical forecast of this process is still far from a final solution. The existing models of heat and mass transfer and deformations for numerical forecasting of soil freezing and heaving have not yet found experimental confirmation in terms of quantitative compliance.

For mathematical modeling of the freezing and heaving process, a physical formulation of the problem is relevant, if it takes into account the essential factors of the processes that take place when testing homogeneous samples with fixed boundary conditions. Currently, it is advisable to conduct research under simpler conditions than those that occur in nature, that is, not to take into account the heterogeneity of soils and the variability of external thermodynamic conditions.

The totality of the essential elements of the system and the parameters of the freezing process should be divided into three groups: (a) internal characteristics (mineralogical composition, organic matter content, grain size, density, porosity, total water content, unfrozen water content, ice content, chemical composition and ionic strength of the pore solution; thermal, mass transfer, and mechanical properties); (b) external factors (the nature of heat exchange and mass transfer, mechanical, hydraulic, and pneumatic effects on the freezing soil and ways to set them in the experiment); and (c) the observed parameters of internal processes of freezing and heaving (temperature and pore pressure distribution, thermal and mass flows, the nature of deformations and ice release, and so on).

CHARACTERISTICS OF KAOLINITE CLAY AS A MODEL SOIL

For physical modeling, a pulverized kaolinite clay was chosen, because of the fact that it is a striking representative, even a standard, in a series of heaving soils. The results of determining the particle-size and microaggregate-size compositions, analysis of water extract, moisture conductivity coefficients, and thermal conductivity of kaolinite clay in thawed and frozen states, as well as the unfrozen water content and starting point of freezing are presented in Tables 1–3 and, Fig. 1. The maximum molecular water capacity of kaolinite clay W_{MWC} is 20.6%; the liquid limit W_L is 45.8%; the plastic limit W_ρ is 34.0%; the plasticity index I_ρ is 11.8%; the solid phase density ρ_s is 2.72 g/cm^3; the initial water content W is 42%; and the compression load is 0.3 MPa. Methods for determining special characteristics (except for the routine methods for determining particle-size distribution and composition of water extract) are described in [*Cheverev, 2004*].

Table 1. **Particle-size and microaggregate-size (in parentheses) distributions in the kaolinite clay sample**

Geol. symbol	Sampling site	Fraction size, mm; fraction content, %								Texture (V.V. Okhotin's classification)
		>0.5	0.5–0.25	0.25–0.1	0.1–0.05	0.05–0.01	0.01–0.005	0.005–0.001	<0.001	
eP_2	Chelyabinsk region, Novokaolinovyi city	0.7 (1.5)	0.5 (0.2)	0.4 (0.2)	2.9 (1.2)	19.5 (32.2)	11.2 (24)	40.2 (34.5)	24.6 (6.2)	Silty clay

Table 2. **Analysis of water extract from kaolinite clay**

pH	Ion content, meq/100 g clay							TDS, %
	HCO_3^-	Cl^-	SO_4^{2-}	Ca^{2+}	Mg^{2+}	K^+	Na^+	
6.9	0.125	0.075	0.407	0.100	0.100	0.019	0.370	0.051

Table 3. **Dependence of the freezing temperature of water-saturated kaolinite clay on density and water content**

Sample no.	Weight water content, u.f.	Density, g/cm^3	Temperature of the beginning of freezing, °C
1	0.36	1.82	–0.26
2	0.39	1.78	–0.24
3	0.42	1.76	–0.16

Figure 1 demonstrates that the dependence of the moisture content of kaolinite clay due to unfrozen water is of a standard character. The temperature of the beginning of freezing depends on the density of the clay and naturally decreases with clay compaction (Table 3).

The analysis of the dependence of the thermal conductivity of clay on the temperature during the transition from the thawed to the frozen state of the soil and back is more complex. In the positive area, the dependence is linear, since it is completely determined by the linear dependence of the thermal conductivity of water on temperature (Fig. 2).

Further, as the soil cools, beginning from the start point of the clay freezing, the appearance of ice due to a decrease in the specific water content significantly increases the thermal conductivity to a peak value. This is due to a fourfold increase in the thermal conductivity of ice (2.2 W/(m·K)) relative to water (0.55 W/(m·K)).

Further cooling from temperature of the completion of the intensive phase transition of water in the clay pores into ice leads to a decrease in thermal conductivity, which is explained by the formation of microcracks.

The temperature reversal, when approaching the area of intense phase transitions, leads to the filling of microcracks of frozen soil with unfrozen water, which restores the high values of thermal conductivity. With a further increase in the temperature of frozen clay, the decrease in thermal conductivity occurs due to a sharp drop in the ice content of the soil and an increase in the content of unfrozen water.

Figure 3 shows the dependences of the moisture conductivity of kaolinite clay in the thawed state on the gradient of pore (hydraulic) water pressure. The method of determination is described in detail in [*Cheverev, 2004*]. Experimental data indicate that, upon small gradients of hydraulic pore pressure (less than 87 m/m), there is a threshold gradient of mois-

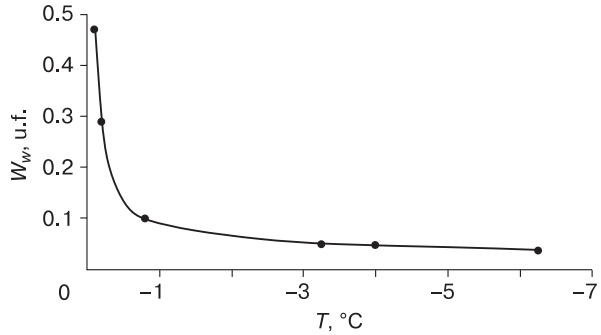

Fig. 1. Dependence of the unfrozen water content of (W_w) frozen silty clay of kaolinite composition on temperature (T) determined by desorption method [*Cheverev et al., 2005*].

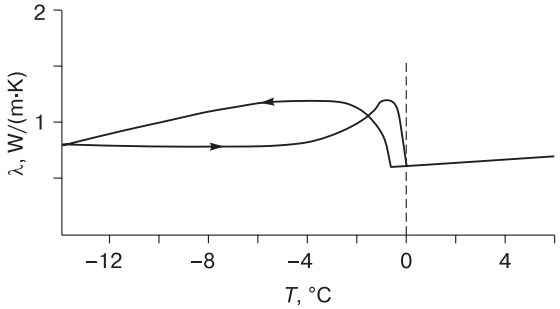

Fig. 2. Dependence of the thermal conductivity coefficient (λ) on the temperature (T) of water-saturated kaolinite clay in the freezing–thawing cycle as determined by the method of stationary thermal regime [*Cheverev, 2004*].

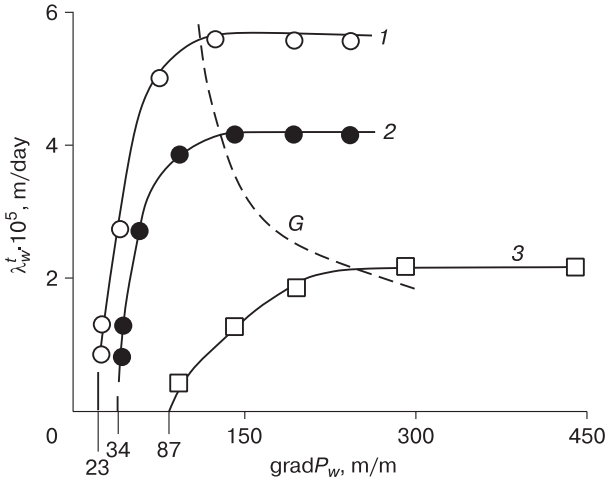

Fig. 3. Dependence of the moisture conductivity coefficient of thawed kaolinite clay (λ_w^t) on the pore pressure gradient (grad P_w) at different densities ρ_d:

(*1*) 1.24, (*2*) 1.3, and (3) 1.42 g/cm^3. *G* is the grad P_w boundary between the linear and nonlinear moisture transfer law.

ture transfer of pore water. As can be seen from the experimental data, the threshold gradient increases with compaction of the clay, namely: at a density of 1.24 g/cm^3, 23 m/m; at 1.30 g/cm^3, 34 m/m; and at 1.42 g/cm^3, 87 m/m. With an increase in the pressure gradient (pressure), the moisture conductivity of clay increases reaching a constant value at pressure gradients characteristic of a particular clay, its temperature and density, and only then Darcy's linear law begins to be fulfilled.

In the frozen zone of the freezing soil, non-compliance with Darcy's law within the limits of the accuracy of determination has not been experimentally established (Fig. 4). In the freezing zone of the soil, a change in the temperature gradient and, accordingly, the pore pressure gradient, while maintaining the average temperature, does not change the proportionality of the cryogenic migration flow density and the pore pressure gradient calculated by Eq. (1).

$$I_w = \lambda_w \, \text{grad} \, P_w, \qquad (1)$$

where λ_w is the soil moisture conductivity coefficient, m/s; I_w is the flow density of cryogenic water migration in the soil, m/s; grad P_w is the gradient of hydraulic pore pressure, m/m. Pressure P_w is measured in meters of water column (1 atm. is equal to 10.33 m of the water column). This pressure dimension is more convenient than Pa and is widely used in agrophysics in describing the thermodynamics of soil moisture and in hydrogeology.

With a decrease in the temperature of clay in the negative area, the moisture conductivity decreases sharply, qualitatively corresponding to the dependence of soil moisture due to the unfrozen water content on temperature [*Cheverev, 2004*].

METHODS OF PHYSICAL MODELING

The purpose of the experimental studies was to examine the parameters of freezing and heaving of soils by laboratory physical modeling. The obtained data were later used to describe the physical formulation of the problem of mathematical modeling of the process taking into account heat and mass transfer and its verification by a preliminary one-dimensional mathematical model [*Cheverev et al., 2021a,b*].

The task of experimental studies was to determine the boundary conditions of the process of freezing and heaving of clay, the dynamics of the temperature field, the movement of the freezing front, the flow of cryogenic migration, deformation of the frost heaving of the freezing zone and shrinkage of the thawed zone, and the parameters of the formation of cryogenic texture recorded by time-lapse video.

The process parameters and characteristics of the clay were set as follows: one-dimensional freezing with fixed boundary conditions for temperature and with an open system for moisture exchange, initial

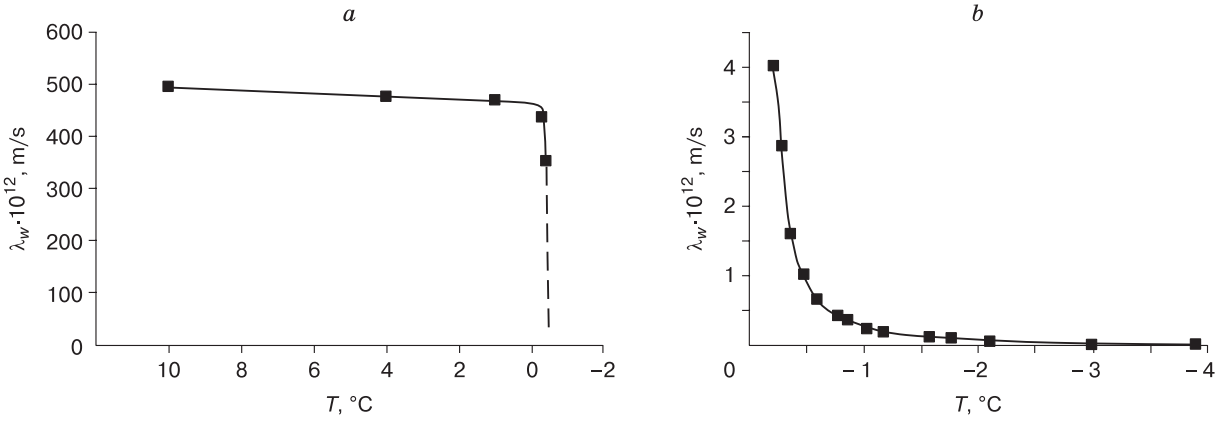

Fig. 4. Dependence of the moisture conductivity coefficient (λ_w) of kaolinite clay in (*a*) thawed and (*b*) frozen states on temperature (*T*).

density and humidity as dependent characteristics of the freezing soil with a full degree of pore filling.

The parameters and characteristics determined were: the distribution of temperature (T) in height and time, pore pressure (P_w), shrinkage and heaving deformation (H_y, H_p), the specific content of unfrozen water (W_w), and the type of cryogenic structure.

To achieve this objective, an automated device was used, the main distinguishing feature of which, giving a significant positive effect, is that soil samples are frozen from the bottom up, and the water supply comes from the top down. A similar scheme of freezing was previously substantiated and successfully used in [*Penner, 1986; Cheverev, 2004; Cheverev et al., 2013*]. In this case, an external load is applied from above from the side of the thawed zone (Fig. 5).

Further, in the description of the equipment, the substantiation of the validity of the application of the proposed methodology for determining the characteristics of frost heaving of soils, including the case of freezing from below, is given.

The device for physical modeling of freezing and heaving of soil (Fig. 5) has the shape of a sleeve with a removable bottom; the soil sample is placed into it. At the upper end of the sample, a capillary-porous stone is placed in an inverted glass with the bottom equipped with a fitting for supplying water and forming pressure in it, unlike atmospheric pressure, in one direction or another, if necessary.

For layer-by-layer measurement of deformations, needle position sensors are installed into the soil at 10 × 10 mm grid. The location of needle position sensors is fixed in time during video shooting. Strain gauges for measuring negative pore pressure in the thawed zone of freezing soil are introduced through the side wall of the sleeve. The strain gauges with a ceramic porous disk and a tube filled with degassed water are provided from the end. The device also includes cooling and load systems not shown in the figure, as well as a control and management automation unit.

The device works as follows. A soil sample is loaded into the sleeve, in the side wall of which, according to a 1 × 1 cm stencil, needle-position sensors are placed to track changes in the density and water content of the soil sample. A capillary-porous stone saturated with water (burnt carborundum or sintered fine-grained sand) is supplied to the soil sample in the glass. A preset load is applied to the bottom of the glass. A water supply system is connected to the fitting for the water supply of the sample through a porous stone.

Water in a porous stone during the experiment is guaranteed to be in a capillary-suspended state. This excludes its gravitational runoff into the soil sample. At the same time, both increased and decreased pressure can be supplied through the fitting, simulating both the pressure of the aquifer and the hydraulic resistance of the thawed zone, or neutral atmospheric pressure, which is equal to zero. Such boundary conditions are possible in nature during soil freezing and therefore were provided by the construction.

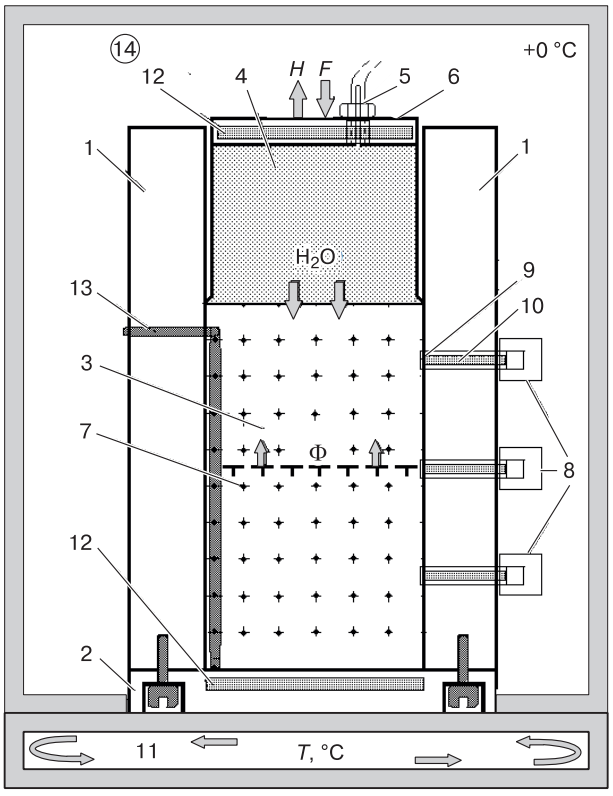

Fig. 5. A device for physical modeling of freezing and heaving of soil with control of boundary conditions and determination of process parameters.

1 – sleeve, 2 – bottom of the sleeve, 3 – soil sample, 4 – capillary-porous stone (or fine-grained sand), 5 – fitting for supply of water and pressure formation in it, 6 – bottom of the cup, 7 – position sensors (tags), 8 – strain gauges of pore hydraulic pressure, 9 – ceramic porous disk at the end of the sensor, 10 – tube with degassed water, 11 – cooling (freezing) zone, 12 – heat flow sensor, 13 – string of thermal sensors, 14 – zero temperature zone; H – heaving vector, F – static load vector, F – freezing front position, H_2O – water in capillary-saturated sand; arrows indicate the direction of water movement into the freezing sample from an external source.

To control the movement of the freezing front in the ground, a garland of thermal sensors is installed on the inside of the sleeve.

The load on the freezing soil sample is carried out through the force sensor by the pneumatic drive unit. Pressure control is carried out by the automated control system. The total pressure in the system is created by means of a compressor.

The theoretical substantiation of the applicability of determining the degree of frost heaving of the soil by freezing the test sample from below is supported by comparative experiments [*Cheverev et al., 2013*].

RESULTS OF PHYSICAL MODELING

Figure 6, as an example, presents the results of freezing the same sample of kaolinite powdery clay obtained during testing with time-lapse shooting: at the beginning of the experiment 0 h and after 20 h.

Moisture-saturated samples of kaolinite clay with the water content of 42% were prepared for the experiment. The samples were placed in sleeves having a parallelepiped shape, in which they were compacted at a load of 0.3 MPa during a week before freezing.

Four freezing experiments were carried out: experiments 2, 3, 4 and 5; each sample during the test had its own characteristics in terms of boundary conditions. In the case of experiment 2, the temperature at the upper and lower ends of the sample was maintained constant (+2 and –1.5°C, respectively) for 36 h; after this, the conditions were changed and new values were set: +1.7 and –3°C, respectively. The remaining experiments did not have such significant changes: for experiment 3, these temperatures were +0.9 and –3.2°C, respectively; for experiment 4, +0.9 and –4.9°C; for experiment 5, +0.5 and –7°C. Unlimited water supply was carried out to the samples, except for experiment 3. In the latter experiment, it was decided to leave for heaving only the volume of moisture that was in the layer of water-saturated sand from above, holding it due to capillary forces. In addition, the samples had different initial heights: experience 2, 150 mm; 3, 121 mm; 4, 103 mm; and 5, 121 mm.

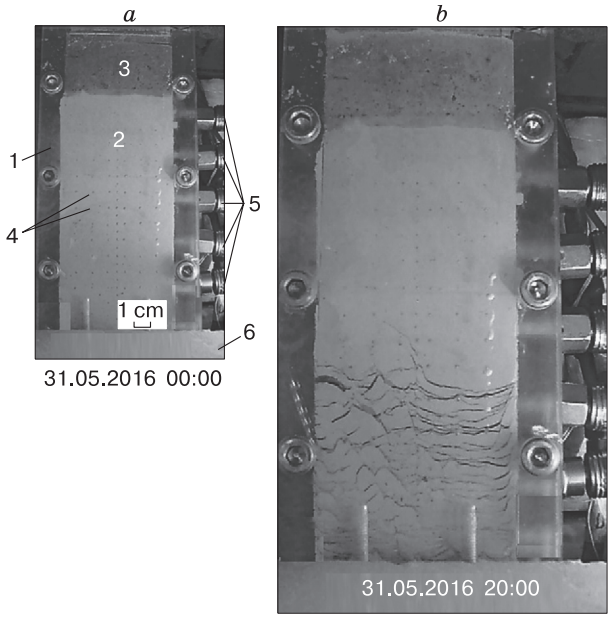

Fig. 6. Experiment 2. Kaolinite clay sample before freezing (*a*) and 20 hours after freezing (*b*).

1 – sleeve, 2 – kaolinite clay sample, 3 – fine-grained sand capillary-saturated with water, 4 – position sensors (tags), 5 – pore pressure sensors, 6 – cooling thermal plate.

During the experiments, pore pressure was measured using built-in sensors along the height of the sleeve, temperature and heat flow density were measured at the upper and lower ends of the sample (Fig. 6).

To track the evolution of the cryogenic structure. the course of the experiment was continuously recorded on the camera. Examples of such evolution during the experiment with an open moisture exchange system at the initial water content of 42% are presented in Fig. 7.

By using time-lapse video recording, the dynamics of segregation ice formation in the freezing soil, layered axial and horizontal deformation (heaving and shrinkage), as well as the dynamics of density and water content of the sample over time. along the height and width of the sample, were obtained. During the cooling of the clay sample, the rate of the freezing front movement naturally slows down, since the temperature gradient decreases with an increase in the height of the frozen zone under fixed boundary conditions.

As a result, the optimum freezing rate for the formation of the largest ice layers and heaving (0.01–0.02 m/day). The cryogenic structure gradually changes from massive and fine-grained to medium- and large-grained. With the maximum deceleration of the movement of the freezing front, the largest ice lenses grow; when the critically low speed of the front movement is reached, the growth of the lenses near it stops. This conclusion logically follows from the established fact that at small gradients of pore pressure (less than 87 m/m) there is a threshold gradient of moisture transfer of pore water (Fig. 3). As a result, cryogenic migration to the freezing front stops. Further extremely slow cooling of the soil may be accompanied by the formation of only a massive cryogenic structure.

Tracing the layered axial and horizontal deformation, as well as the dynamics of the sample density over time, in height and width of the sample showed the following. In the freezing soil, the outflow of water from the thawed zone into the frozen zone causes a decrease in pore pressure in it. As a result, the thawed zone experiences volumetric shrinkage. During freezing, the shrinkage zone lengthens and becomes the zone of transit transfer of water from an external source to the freezing zone. In this case, the density and water content of the shrinkage limit is achieved, which is close to the lower limit of plasticity of kaolinite clay [*Cheverev, 2004*].

As the height of the samples was different, different values given were used as evaluation characteristics. For example, Fig. 8 presents the results of changes in the relative deformation of samples over time (e), which was calculated by the formula:

$$e = (H - H_0)/H_0,$$

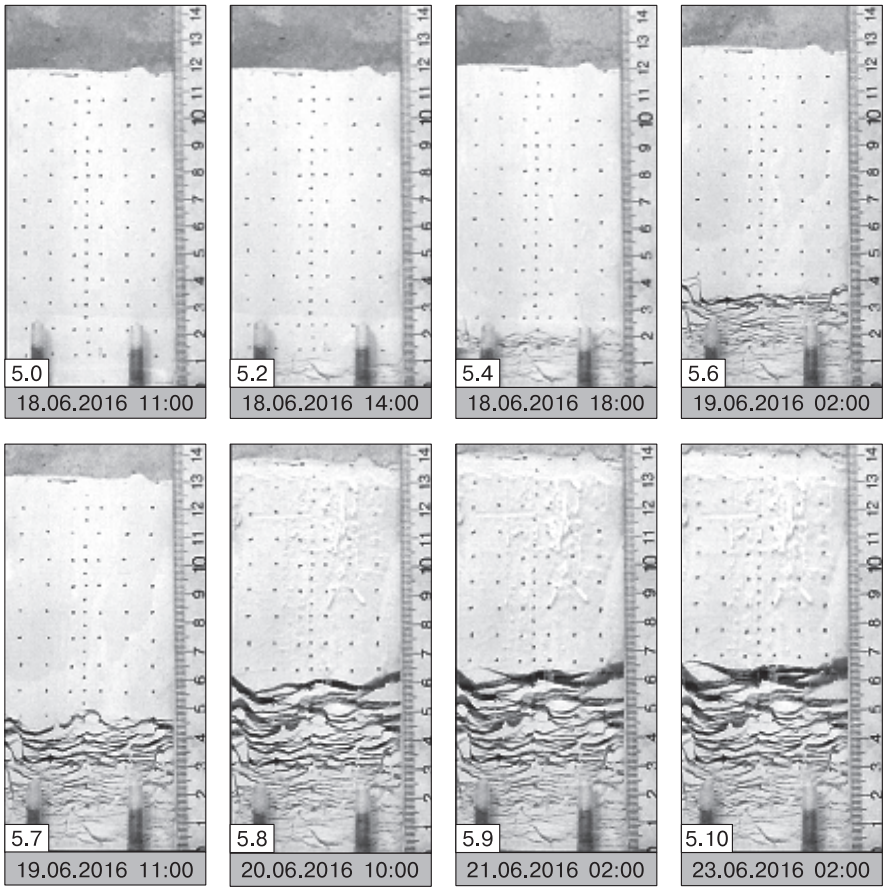

Fig. 7. Experiment 5. Fragments of the dynamics of cryogenic structure formation in a sample of kaolinite clay at different points in time.

5.0–5.10, laboratory numbers of time-lapse photos. State of the sample before the beginning of freezing at 11 a.m. on June 18, 2016.

where H_0 is the height before freezing, and H is the height during freezing.

The change in the height of the frozen layer over time was calculated on the basis of camera data, on which the boundary of the thawed and frozen zones was clearly visible even in the absence of ice lenses in the transition zone ("freezing edge"), where the massive cryogenic structure is observed: the frozen part of the soil sample in the vicinity of the freezing front was darker compared with the thawed part.

Figure 9 shows the change in the proportion of the frozen part of the total height of the freezing samples over time.

Tracking the frozen part made it possible to calculate the relative heaving deformation (ε_{fh}) of samples over time (Fig. 10) using the formula:

$$\varepsilon_{fh} = h_f/d_i,$$

where h_f is the vertical deformation of the soil sample at the end of the test, mm; d_i is the thickness of the frozen layer of the soil sample minus h_f, mm.

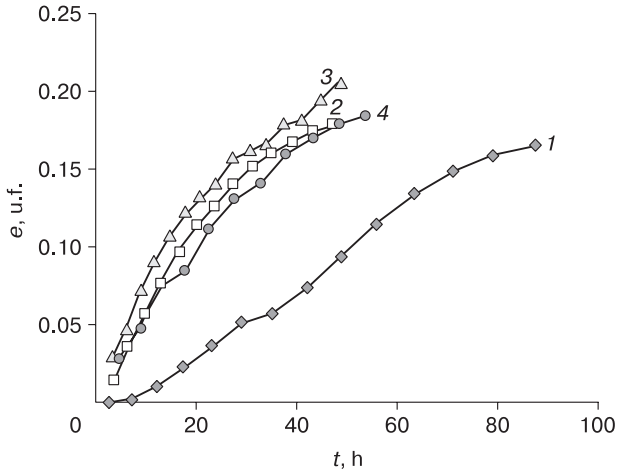

Fig. 8. Change in the relative deformation of freezing samples (e) over time (t) under different temperature boundary conditions.

1 – experiment 2, T = +2, –1.5°C up to 30 h and T = +1.7, –3°C after 36 h; *2* – experiment 3, T = +0.9, –3.2°C; *3* – experiment 4, T = +0.9, –4.9°C; *4* – experiment 5, T = +0.5 и –7°C.

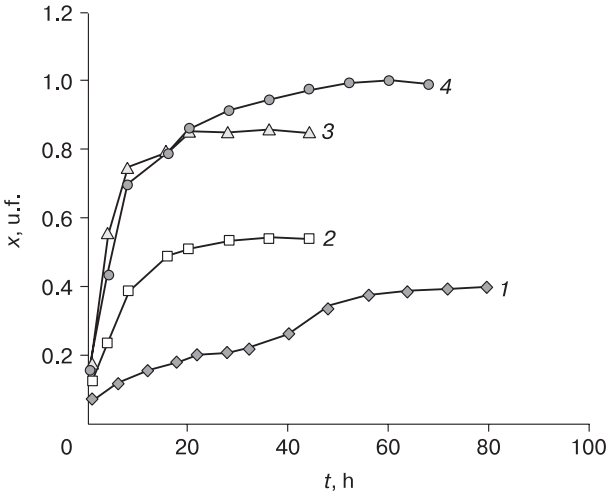

Fig. 9. Change in the relative fraction of the frozen part from the total height of the freezing samples (x) over time (t) under different boundary conditions.

(*1–4*) see Fig. 8.

In Fig. 9, one can note a significant acceleration of the freezing process and an increase in the proportion of the height of the frozen part in the sample, when the boundary conditions change from the cold part towards lower temperatures. Interestingly, the dynamics of deformation of a freezing sample with the lowest temperature of the cold zone –7°C (experiment 5), as can be seen from Fig. 8, is comparable with freezing samples at a higher corresponding boundary temperature (experiments 3 and 4), while the freezing sample in experiment 2 with the highest boundary temperatures is noticeably behind them.

At the same time, the sample in experiment 5 has the lowest dynamics of heaving, and the sample in experiment 2 has the highest one (Fig. 10). This is primarily due to the fact that the sample in experiment 5 froze much faster than in experiment 2 (Fig. 9). As a result, due to too fast freezing, the high initial values of the water flow in the ground in experiment 5 were leveled and rapidly decreased, while the value of the water flow in experiment 2 kept a high value (Fig. 11).

The dynamics of freezing of the sample in experiment 5, as the authors believe, is associated with the prevailing expansion of the soil in this case due to the freezing of water that was in its pores initially. The contribution to the expansion of the soil in this experiment due to the growth of ice lenses is minimal in comparison with other samples, which is further confirmed by the low values of the water flow during the test (Fig. 11). At the same time, for the sample in experiment 2, in the "warmest" conditions, the contribution to the expansion of the soil due to the growth of ice lenses plays the dominant role, which is reflected in Figs. 10 and 11.

Figure 12 shows graphs of changes in heat fluxes over time (I_q), with "cold" and "warm" denoting the lower and upper ends of the sample, respectively.

The heat flow density was measured at the upper and lower ends of the sample, while negative temperature was applied to the lower end, and positive temperature was applied to the upper end.

The pore pressure sensors in the samples worked stably only for the first 6 to 9 h, and this is normal. During this time, bubbles gradually formed inside the sensors due to a decrease in pressure from the air dissolved in water, after which the sensor could not correctly measure the pore pressure. The lower the pres-

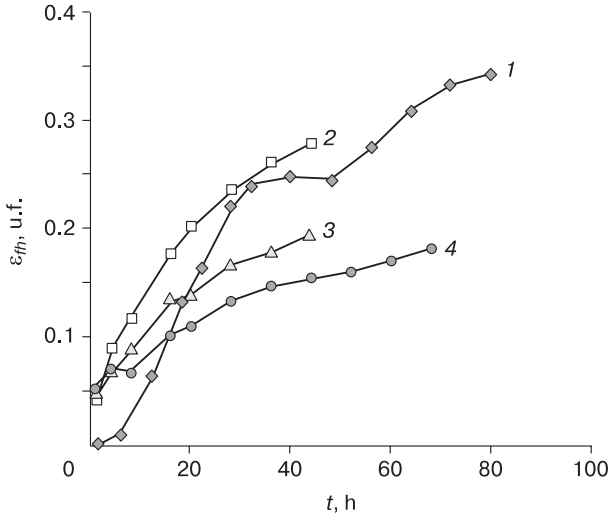

Fig. 10. Changes in the relative heave deformation (ε_{fh}) of samples over time (t) under different boundary conditions.

(*1–4*) see Fig. 8.

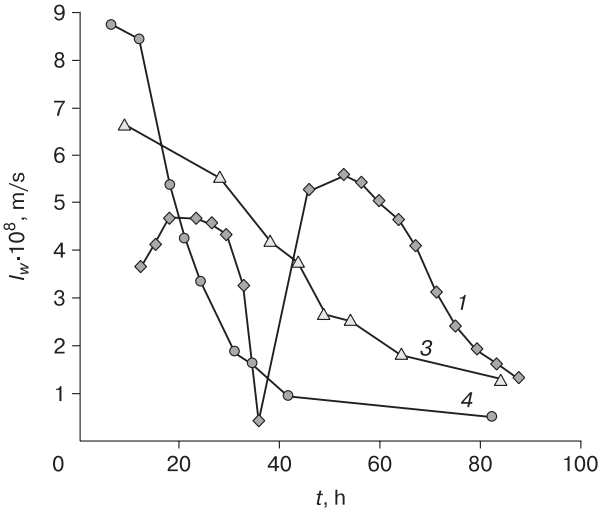

Fig. 11. Changes in the soil water flow density (I_w) in the samples as a function of time (t) under different boundary conditions.

(*1–4*) see Fig. 8.

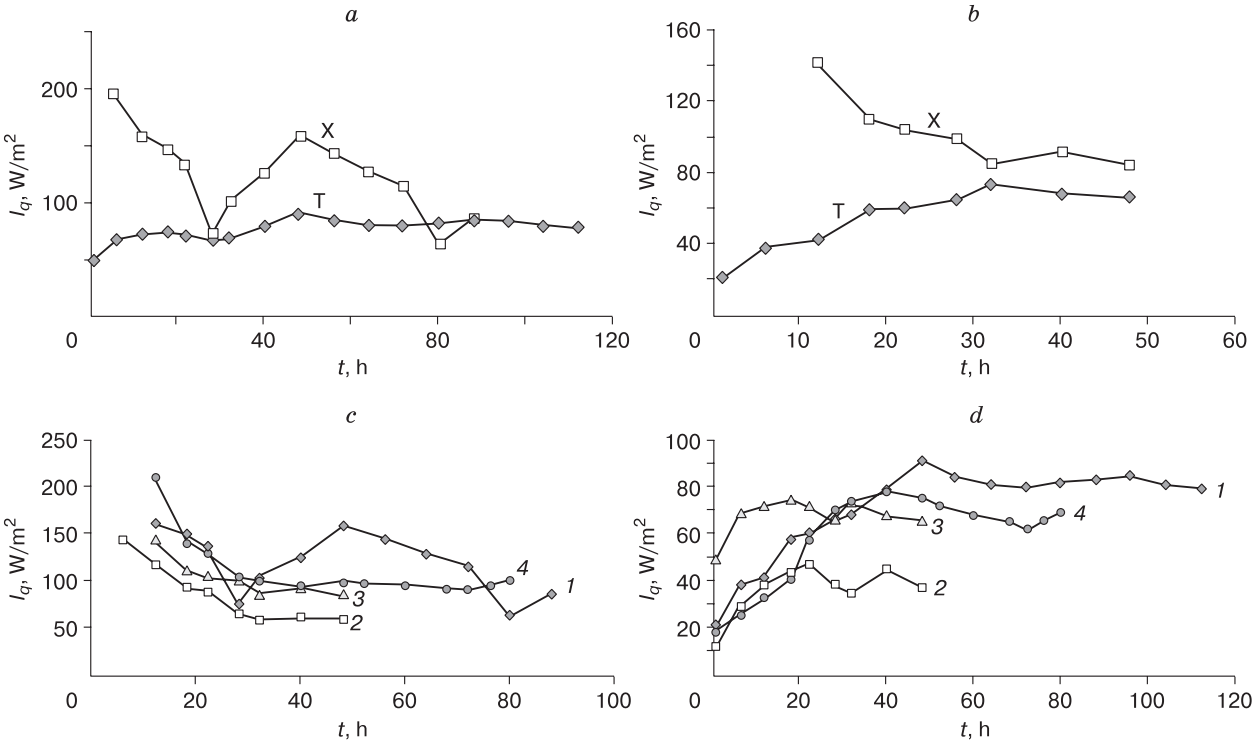

Fig. 12. Changes in the density of heat fluxes (I_q) over time (t) in the freezing kaolinite clay sample:

(*a*, *b*) heat fluxes at the warm (T) and cold (X) ends during freezing of the sample in experiments 2 and 4, respectively; (*c*) heat fluxes at the warm end face; and (*d*) heat fluxes at the cold end face. (*1*–*4*) see Fig. 8.

sure, the faster this process. When the sensor froze, the reverse process occurred, that is, the freezing of water in the sensor increased the pressure in it to 12 atm or more. That is, for this type of sensors made of baked kaolinite clay, there is a natural measuring range of negative pressure no lower than –0.8 atm. To measure lower pressures, as well as for measurements in saline freezing soils, it is necessary to use osmometers, which, unfortunately, are not yet technically developed enough to measure pore pressure in freezing soils.

As can be seen from the experimental data (Fig. 13), the distribution of pore pressure along the height of the freezing soil in its thawed zone is close to linear, which indicates the filtration mechanism of moisture transfer.

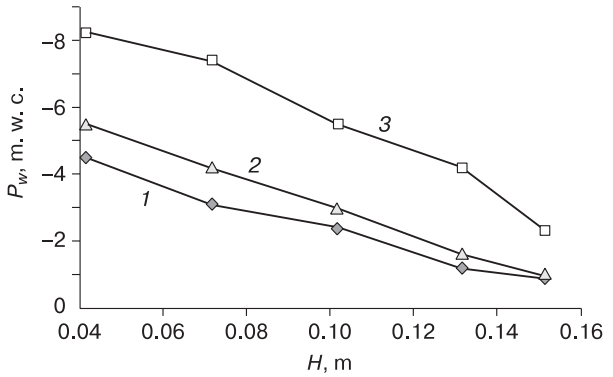

Fig. 13. Pore pressure profile in the thawed zone (P_w) by the height (H) of the kaolinite clay sample at different time moments during freezing (experiment 2).

1 – 1 h, *2* – 3 h, and *3* – 6 h.

CONCLUSIONS

1. Physical laboratory modeling of the freezing of kaolinite clay composition, which belongs to strongly heaving soils, was performed. The main characteristics of the component and phase composition of water in the model clay, as well as its heat and mass transfer and deformation properties were determined. During the physical modeling, the parameters of the freezing process, differential heaving of frozen and shrinkage of thawed zones, heat and moisture transfer and pore pressure of water were monitored.

2. By using time-lapse video, the dynamics of segregation ice release in the freezing ground, layered axial and horizontal deformation (heaving and shrinkage), as well as the dynamics of the density (moisture content) along the sample height over time were revealed.

3. A change in the boundary conditions, namely a sudden decrease in temperature from the cold source, first led to a sharp slowdown in the deformation and heaving of the sample and the process of moisture transfer to the freezing front, and then, conversely, accelerated these processes.

4. The freezing of samples in a certain range of boundary conditions led to comparable dynamics of the heaving of samples; however, the freezing rates varied significantly, which ultimately resulted in different final heaving deformation after the freezing front in the sample was practically stopped.

5. The filtration mechanism of moisture transfer in the thawed zone of the freezing highly porous soil was experimentally confirmed.

Acknowledgments. *The materials for this paper were obtained with financial support of Transneft Research Institute LLC (contract no. 4220 P/20-511/2015 from November 19, 2015.*

References

Cheverev V.G., 2004. *The Nature of Cryogenic Properties of Soils.* Moscow, Nauchnyi mir, 234 p. (in Russian).

Cheverev V.G., Brushkov A.V., Polovkov S.A. Pokrovskaya E.V., Safronov E.V., 2021a. Analysis of concepts on the mechanism of cryogenic water migration in freezing soils. *Earth's Cryosphere* XXV (5), 3–10.

Cheverev V.G., Burnaev R.S., Gagarin V.E., Safronov E.V., 2013. Influence of the external pressure on the degree of frost heaving of clay soils. *Kriosfera Zemli* XVII (4), 57–62 (in Russian).

Cheverev V.G., Safronov E.V., Korotkov A.A., Cherniatyn A.S., 2021b. Physical formulation of the numerical modeling of freezing and frost heaving of soils with consideration of heat and mass transfer. *Nauka Tekhnol. Truboprovodn. Transp. Nefti Nefterpoduktov* **11** (3), 244–256 (in Russian).

Cheverev V.G., Vidyapin I.Yu., Motenko R.G., Kondakov M.V., 2005. Determination of the content of unfrozen water in soils by sorption-desorption isotherms. *Kriosfera Zemli* IX (4), 29–33 (in Russian).

Garagulya L.S., Buldovich S.N., Romanovsky N.N. et al., 2000. Geocryological hazards. In: *Natural Hazards of Russia*. Moscow, Firm "KRUK", 315 p. (in Russian).

Penner E., 1986. Aspects of ice lens growth in soils. *Cold Reg. Sci. Technol.* **13**, 91–100.

Received July 5, 2022
Revised December 12, 2022
Accepted December 19, 2022

Translated by S.B. Sokolov